Metamorphic pyroxenes from the Broken Hill district, New South Wales.

By R. A. Binns, B.Sc.

Department of Mineralogy and Petrology, University of Cambridge.

[Read 25 January 1962.]

Summary. The Archean rocks of the Barrier Ranges, New South Wales, show zones of progressive regional metamorphism of which the highest is characterized by orthopyroxene-bearing basic granulites. Within this zone, further increase in metamorphic grade results in a detectable change in distribution of ferrous iron and magnesium between coexisting orthopyroxene and clinopyroxene, the latter becoming relatively richer in iron. Mutual solid solution between the two pyroxene phases also appears to increase. The value of coexisting pyroxenes as indicators of metamorphic grade is thus established. There are some points of disagreement between the Broken Hill results and previously advanced theories of cation distribution in pyroxenes.

THE study of mineral assemblages in Archean rocks from the Willyama 'Series' of the Barrier Ranges, far western New South Wales, has revealed a sequence of zones representing their progressive regional metamorphism. Assemblages in members of pelitic and of basaltic composition have proved most useful as markers of metamorphic grade, enabling recognition of three major zones increasing in grade from north-west to south-west across the north-easterly-striking regional structure. In the lowest, most westerly of these zones, basaltic rocks are represented by amphibolites containing a green or blue-green variety of hornblende together with occasional garnet and rarer epidote or clinozoisite, while pelitic rocks are recrystallized to sillimanite- and garnet-bearing muscovite–biotite schists. Amphibolites also characterize the central, intermediate-grade zone but their constituent hornblende now becomes a green-brown or brown-green variety and they may contain clinopyroxene as well as garnet. Pelitic rocks of this zone are orthoclase-bearing sillimanite–garnet–biotite gneisses lacking primary muscovite. The easternmost, highest-grade zone is marked by the appearance of orthopyroxene along with clinopyroxene and hornblende in rocks of basaltic composition. The pelitic gneisses are similar to those of the intermediate zone.

The 'orthopyroxene isograd' marking the transition from intermediate to the highest-grade zone is readily mapped in the field and is apparently unrelated to any major tectonic feature such as faults or crush zones. In terms of the facies classification of Turner (Fyfe, Turner, and Verhoogen, 1958), the three zones denote progression from the sillimanite–almandine–muscovite subfacies of the almandine–amphibolite facies, through the sillimanite–almandine–orthoclase subfacies of the same facies, to the hornblende–granulite subfacies of the granulite facies.

The areal distribution of the three zones is shown on fig. 1. The Barrier Ranges stand isolated in arid, sandy plains and consequently little is known of the nature of the regional metamorphism beyond the three zones described. In the Olary Hills of South Australia, some 50 to 70 miles west-south-west of Broken Hill, pelitic rocks correlated with the Willyama series of the Barrier Ranges have been recrystallized to staurolite- and kyanite-bearing schists and, even farther west, to andalusite-bearing schists, suggesting that the metamorphic grade continues to fall slowly and uniformly westwards from the lowest-grade zone represented in the Barrier Ranges. To the east, exposures of Archean rocks are unknown.

Relationships within the zone of granulites.

Beyond the orthopyroxene isograd, no new mineral assemblages that define further increase in metamorphic grade are found. However, the regularity in distribution of mapped metamorphic zones and their immense scale implies that the overall easterly increase in metamorphic grade must continue for at least some distance beyond the isograd into the zone of hornblende–pyroxene granulites, and it will be possible to correlate distance of a particular locality from the orthopyroxene isograd with its relative metamorphic grade. Evidence in support of this contention, to be presented in a later communication, is provided by continuous variation in the nature of amphibole minerals through the amphibolite zones up to the orthopyroxene isograd, and beyond this well into the granulite zone. Furthermore there are indications that hornblende decreases in importance as a major constituent mineral in granulites as one moves east of the isograd. Certain relationships between coexisting pyroxenes of rocks in the granulite zone have been found to vary with distance from the isograd, that is with the grade of metamorphism, and the purpose of this paper is to present and discuss these observations.

During the preliminary optical examination of mineralogical variation in the Broken Hill pyroxene granulites, refractive indices of orthopyroxene and clinopyroxene were found to vary interdependently in

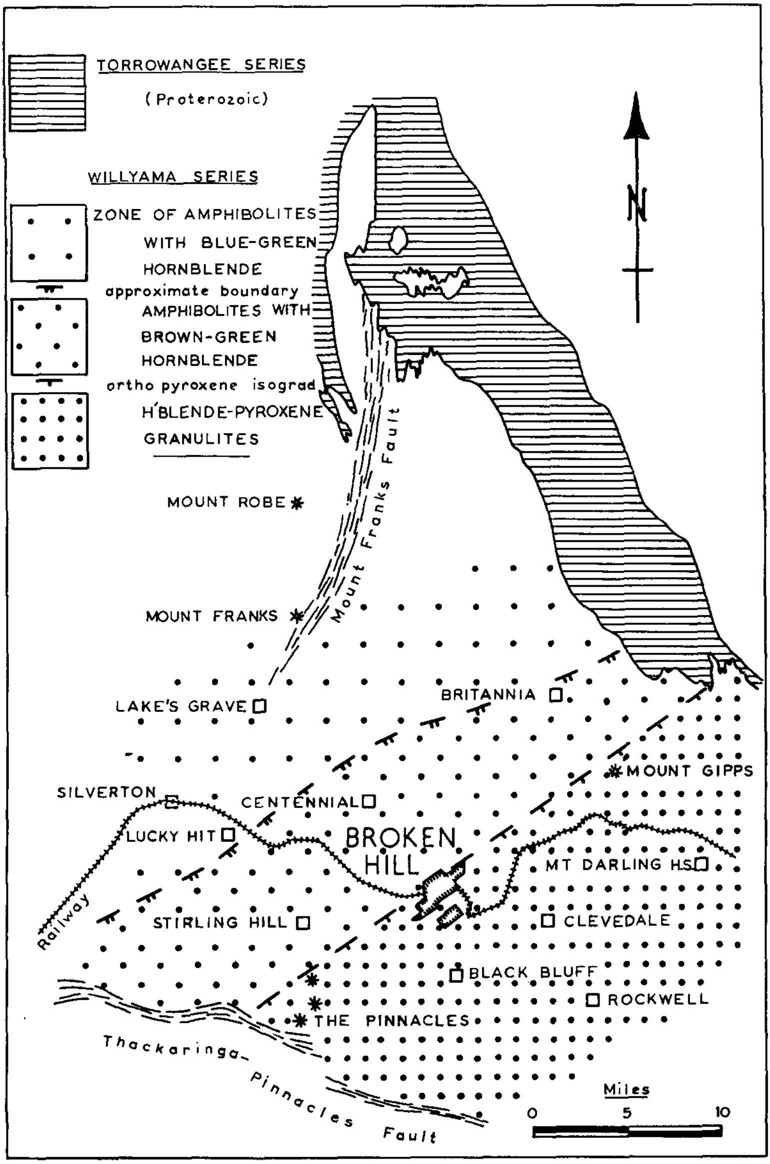

FIG. 1. Map of the Broken Hill district, New South Wales, showing outcrops of the Proterozoic rocks (Torrowangee Series) and the three zones of regional metamorphism in the underlying Archean rocks (Willyama Series). The Willyama–Torrowangee boundary is taken from King and Thompson (1953), Plate III.

such a manner that, on a graphical plot of orthopyroxene index γ against index β of the coexisting clinopyroxene, the resultant points for different specimens from the one locality fall on an inclined straight line. Comparing, then, inclined lines for other localities it was found that while the slopes remain essentially the same, the position of the line upon the graph depends upon the distance of the locality from the orthopyroxene isograd. The data obtained are presented in fig. 2, where it may be seen that specimens from the Pinnacles, from Broken Hill City, and from

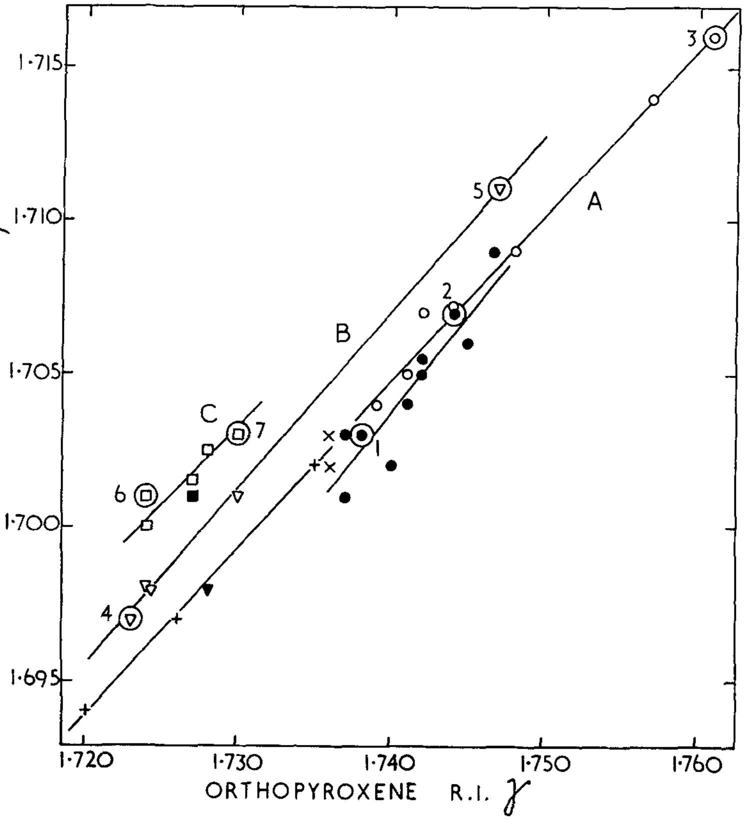

FIG. 2. Plot of refractive index γ of orthopyroxene against β of coexisting clinopyroxene (both ± 0·001). Lines *A*, *B*, and *C* denote the refractive index relationship trends for specimens from the lower-, intermediate-, and higher-grade subzones respectively. Symbols correspond to those by which the localities are marked on fig. 3. Analysed pyroxene pairs are numbered as in table I and shown by large circles.

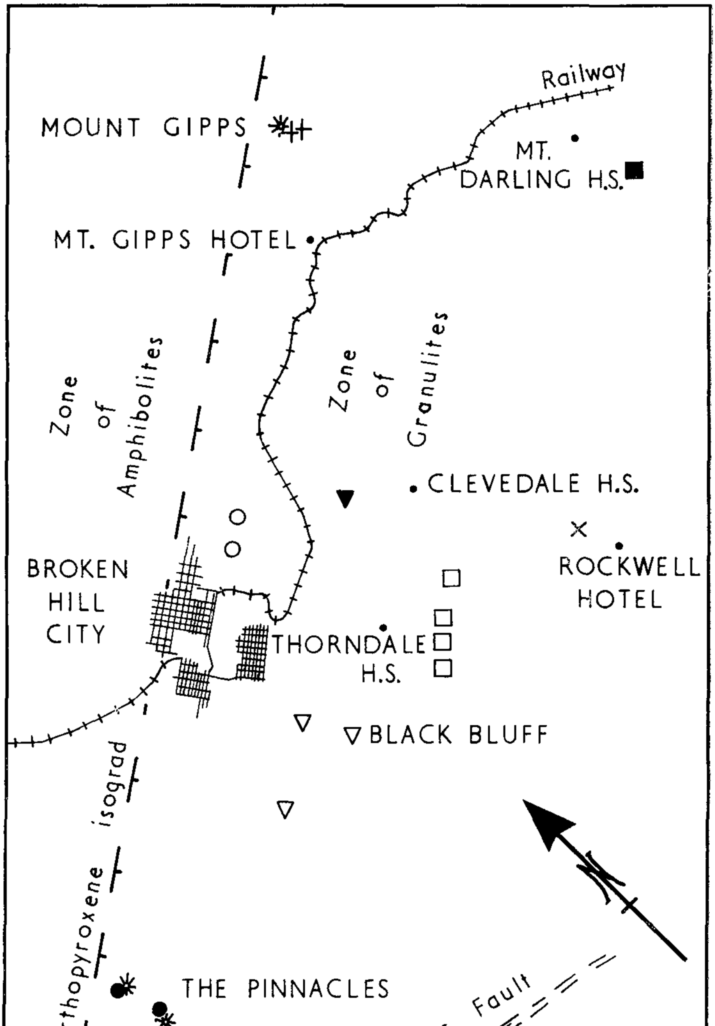

FIG. 3. Map showing localities mentioned in the text.

Mount Gipps (all localities close to the orthopyroxene isograd, 0·5 to 1·6 miles) plot on much the same straight line (line *A*) while specimens from Black Bluff and from east of the White Leads prospect (localities more distant from the isograd, 3·5 to 5 miles) define a similarly-sloping line lying above the first line (line *B*). Clevedale, Thorndale, and Mount Darling Homesteads constitute a third group of localities more distant again from the isograd (6·3 to 9 miles) and specimens from these plot on a line even further displaced from the first line (line *C*).[1]

The zone of hornblende–pyroxene granulites may thus be subdivided on the basis of relationship in the optical properties of coexisting pyroxenes. The three subdivisions corresponding to lines *A*, *B*, and *C* will be referred to as the lower-, intermediate-, and higher-grade subzones of the hornblende–pyroxene granulite zone respectively.

The localities from which specimens plotted on fig. 2 were obtained are distinguished on the map of fig. 3 by corresponding symbols. To determine the factors underlying these differences in coexisting pyroxene relationships, chemical analyses have been performed on selected specimens from the three subzones. These are numbered and denoted by large circles on fig. 2. Three pyroxene pairs from the lower-grade subzone, two from the intermediate- and two from the higher-grade subzones have been analysed (table I). All the specimens are hornblende–pyroxene granulites, although only traces of hornblende exist in specimen 5. All but specimens 4 and 5 contain quartz.

Results of the chemical study.

No progressive change in content of minor components from lower- to higher-grade subzones is revealed by the analyses of either clinopyroxenes or orthopyroxenes; rather the content of manganese, titanium, ferric iron, and aluminium varies in all subzones according to the quantities available in the rock. Aluminium is higher in the pyroxenes from Thorndale, but this is an indirect result of the bulk chemistry of these rocks; their higher alkali content causes a more sodic, less aluminous plagioclase to crystallize, in consequence forcing aluminium into the mafic minerals. Ferric iron is higher in lower-grade clinopyroxene 3 and higher-grade orthopyroxene 7, both from oxidized rocks containing magnetite. Apart from these, the variations in minor components are insufficient to affect optical properties substantially, and

---

[1] Two specimens from Rockwell plotted anomalously, but since these rocks were extensively altered, no significance has been attached to these results. A specimen from the vicinity of Clevedale Homestead also plotted anomalously (see fig. 2).

the lack of progressive changes through the subzones precludes any possibility that the observed variation in optical relationships of coexisting pyroxenes may be explained by changes in the quantities of minor components accepted into the pyroxene structure from one subzone to another, or by a simple change in the oxidation state of iron.

However a very close correlation exists between the refractive index of the orthopyroxenes and their chemically-determined content of total iron plus manganese. A similar though slightly less precise relationship has also been found in the clinopyroxenes discussed in this paper and in other clinopyroxenes from Broken Hill that have been analysed. This implies that variations in the relative concentrations of total iron plus manganese underlie the relationships in optical properties recorded on fig. 2. The absence of progressive or consistent variations in either manganese or ferric iron suggests that changes in ferrous iron content are responsible, in which case the straight line plots of optical properties in fig. 2 would represent an orderly distribution of ferrous iron between the pyroxenes coexisting under environmental conditions pertaining to the different subzones, while the separation of the lines for the different subzones denotes a change in the nature of the distribution relationship corresponding to a change in the environmental conditions.

Such a distributional relationship is best studied by plotting the proportion of ferrous iron in orthopyroxene against that of its coexisting clinopyroxene, physico-chemical principles requiring that this proportion be compared with that of another major component occupying the same site in the pyroxene structures (i.e. magnesium). In fig. 4 the atomic proportion of ferrous iron, $Fe^{\cdot\cdot}/(Fe^{\cdot\cdot}+Mg)$ in orthopyroxene has been plotted against that of clinopyroxene. The line passing through points representing pyroxene pairs 1, 2, and 3 denotes the distribution relationship existing in the lower-grade subzone, that passing through points 4 and 5 denotes the relationship in the intermediate-grade subzone, and that through points 6 and 7 represents the higher-grade subzone.

There is a distinct spacing of the two lines representing the lower- and intermediate-grade subzones, implying a change in the distributional relationship between these zones. The line directly joining points 6 and 7 cuts across the intermediate subzone line (4–5) but for reasons discussed presently the analysis of clinopyroxene 7 may not be representative of its original composition, and it is probable that the true distributional relationship in the higher-grade subzone is denoted by the line shown drawn through point 6 on fig. 4, indicative of further change in the distributional relationship from that in the lower subzones.

TABLE I. Analyses of coexisting pyroxenes. (Analyst, R. A. Binns.)

	Orthopyroxenes							Clinopyroxenes						
	1.	2.	3.	4.	5.	6.	7.	1.	2.	3.	4.	5.	6.	7.
SiO_2	49·34	49·27	47·44	51·13	49·04	50·26	—	51·03	51·05	49·15	51·68	50·47	50·95	50·65
TiO_2	0·18	0·28	0·48	0·29	0·24	0·21	—	0·20	0·25	0·40	0·39	0·39	0·25	0·28
Al_2O_3	1·28	0·23	0·92	0·87	0·89	2·05	—	2·12	1·16	1·47	1·44	1·24	2·40	3·14
Fe_2O_3	0·60	0·09	0·32	0·67	0·57	0·63	1·78	0·75	0·10	1·28	0·55	0·66	0·63	0·26
FeO	32·83	36·55	40·75	28·22	36·86	28·30	28·34	13·08	15·67	21·39	11·32	18·21	11·70	11·85
MnO	1·26	0·87	1·64	0·61	0·72	0·30	0·84	0·49	0·38	0·82	0·26	0·32	0·33	0·26
MgO	13·51	11·98	7·63	17·51	10·88	17·28	15·56	10·73	9·66	6·82	12·70	8·86	12·09	11·81
CaO	0·87	0·82	1·10	0·95	1·36	0·87	0·87	21·28	21·49	19·09	21·54	20·04	20·90	21·30
Na_2O	0·13	0·03	0·21	0·04	0·03	0·03	—	0·39	0·24	0·36	0·30	0·16	0·42	0·40
K_2O	0·04	0·01	0·02	0·01	0·01	0·01	—	0·02	0·01	0·03	0·01	0·01	0·01	0·03
H_2O-	0·00	0·00	0·00	0·02	0·00	0·00	—	0·00	0·00	0·00	0·00	0·00	0·00	0·00
Total	100·04	100·13	100·51	100·32	100·60	100·44	—	100·09	100·01	100·81	100·19	100·36	99·68	99·98
Atomic ratios to 6 oxygen atoms and $z = 2·00$.														
Si	1·952	1·976	1·952	1·962	1·964	1·931	—	1·943	1·968	1·933	1·949	1·956	1·932	1·916
Al^{iv}	0·048	0·010	0·044	0·038	0·036	0·069	—	0·058	0·032	0·067	0·051	0·044	0·068	0·084
Al^{vi}	0·014	0·000	0·000	0·003	0·007	0·023	—	0·038	0·019	0·002	0·012	0·012	0·042	0·057
Ti	0·005	0·010	0·015	0·009	0·007	0·006	—	0·005	0·007	0·012	0·011	0·012	0·007	0·008
Fe^{+3}	0·019	0·002	0·010	0·018	0·017	0·018	—	0·021	0·003	0·038	0·016	0·019	0·018	0·009
Fe^{+2}	1·087	1·226	1·401	0·904	1·235	0·910	—	0·416	0·505	0·704	0·358	0·591	0·372	0·375
Mn	0·043	0·029	0·057	0·021	0·024	0·025	—	0·016	0·012	0·028	0·007	0·012	0·011	0·008
Mg	0·797	0·716	0·467	1·001	0·650	0·988	—	0·608	0·556	0·399	0·714	0·510	0·684	0·666
Ca	0·036	0·036	0·047	0·039	0·058	0·036	—	0·868	0·887	0·803	0·870	0·834	0·851	0·864
Na	0·005	0·001	0·017	0·004	0·003	0·002	—	0·027	0·018	0·028	0·023	0·014	0·032	0·032
K	0·002	0·000	0·000	0·000	0·000	0·000	—	0·001	0·000	0·001	0·000	0·000	0·000	0·001
$X+Y$	2·008	2·020*	2·014†	1·999	2·001	2·008	—	2·000	2·007	2·015	2·011	2·004	2·017	2·020
Ca	1·9	1·8	2·4	2·0	2·9	1·8	1·9	45·0	45·2	41·0	44·3	42·4	44·0	45·0
Mg	40·2	35·6	23·6	50·4	32·8	50·0	46·6	31·5	28·2	20·0	36·3	26·0	35·3	34·7
ΣFe	57·9	62·6	74·0	47·6	64·3	48·2	51·5	23·5	26·6	39·0	19·4	31·6	20·7	20·3
$Fe^{\cdot\cdot}/Mg^{\cdot\cdot}$	1·364	1·716	3·002	0·906	1·896	0·921	1·022	0·684	0·912	1·785	0·501	1·160	0·544	0·562
$Fe^{\cdot\cdot}/(Fe^{\cdot\cdot}+Mg^{\cdot\cdot})$	0·577	0·632	0·750	0·475	0·655	0·479	0·505	0·406	0·477	0·641	0·334	0·537	0·352	0·360

* $z = 1·986$. † $z = 1·996$.

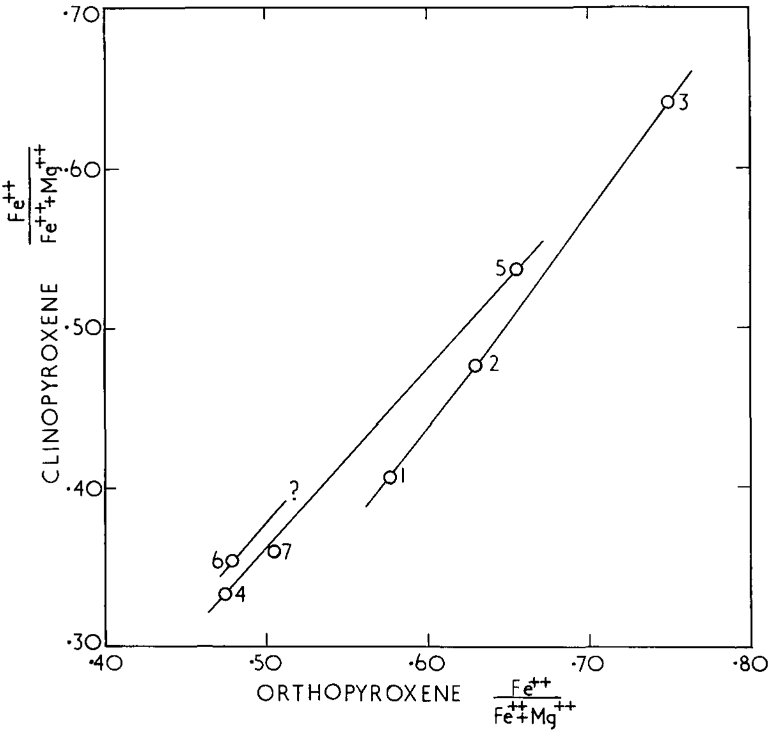

FIG. 4. Distribution diagram on which the atomic ratio Fe˙˙/(Fe˙˙+Mg) of orthopyroxene is plotted against that of its coexisting clinopyroxene. The lines passing through pyroxene pairs 1, 2, and 3; 4 and 5; and through 6 represent distribution trends in the lower-, intermediate-, and higher-grade subzones respectively. The diameter of the circles by which the various points are marked corresponds roughly to the maximum likely analytical error.

Key to table I.

1. opx–cpx–hb–plag–qtz–ilm granulite [84319], ½ mile NE. of Middle Pinnacle, The Pinnacles.
2. opx–cpx–hb–plag–qtz–ilm granulite [84320], ½ mile NE. of Middle Pinnacle, The Pinnacles.
3. opx–cpx–hb–plag–qtz–mt–ilm granulite [84321], D.D. hole 503, 598 ft from collar, North Mine, Broken Hill.
4. opx–cpx–hb–plag–ilm granulite [84322], western side of Black Bluff.
5. opx–cpx–plag–ilm granulite, locally with traces of hornblende [84323], eastern side of Black Bluff.
6. opx–cpx–hb–plag–qtz–mt–ilm granulite [84324], 2 miles east of 'Thorndale' homestead.
7. opx–cpx–hb–plag–qtz–mt–ilm granulite [84325], 2 miles east of 'Thorndale' homestead (partly altered specimen).

Specimen numbers apply to the collection in the Department of Mineralogy and Petrology, Cambridge. All specimens contain traces of apatite; opx = orthopyroxene, cpx = clinopyroxene, hb = hornblende, plag = plagioclase, qtz = quartz, mt = magnetite, ilm = ilmenite.

As may have been anticipated from the relationship between composition and optical properties discussed above, there is a marked correspondence between the chemical plot of fig. 4 and the comparable points representing the analysed pairs on the optical plot of fig. 2.

The specimen from which pyroxene pair 7 was obtained was rather altered and during separation it was found necessary to treat the material with acid. This treatment tended to remove iron-rich alteration products of exsolution lamellae within clinopyroxene and has probably affected the iron–magnesium ratio of clinopyroxene 7 and brought about anomalous plotting of pair 7 upon fig. 4. The effect upon refractive index of their relative alumina content probably accounts for the diminished spacing on the chemical plot as compared to the optical plot between the lines representing pyroxene pairs from the intermediate-grade and higher-grade subzones respectively.

With regard to analytical precision and its effect on the validity of the foregoing interpretation of fig. 4, a pessimistic estimate of the accuracy of ferrous iron oxide and magnesia determinations (0·2 weight per cent of the mineral in each case) leads to a maximum error in the position of a point on fig. 4 roughly equivalent to the radius of the circles by which points representing pyroxene pairs have been denoted on that diagram. The actual errors are probably less than this. Taking this likely accuracy into account and recalling the relative abundance and consistency of the optical data, it may be confidently deduced from the chemical analyses that with increase in metamorphic grade through the several subzones there has been a change in the manner in which ferrous iron and magnesium have been distributed between the two coexisting pyroxene phases of the metamorphosed basic rocks.

Some information concerning distribution of minor components between orthopyroxene and clinopyroxene is also available from the analyses. Manganese is distributed very regularly, the ratio of the total atomic fraction in orthopyroxene to that in clinopyroxene averaging 1·36, with no detectable differences between the three subzones. In the lower-grade specimens titanium tends to be relatively less concentrated in clinopyroxene than in the higher grades, although the quantities are small and the differences slight. With regard to aluminium, analytical accuracy permits only the statement that this constituent is relatively concentrated in the clinopyroxene. Measurement of ferric iron content is also subject to analytical error, but there is a definite suggestion that in the higher subzones orthopyroxene accepts ferric iron cations more readily compared with its coexisting clinopyroxene than it does in the lower-grade subzones.

A triangular plot of calcium, magnesium, and total iron plus manganese (ΣFe) provides a convenient representation of pyroxene com-

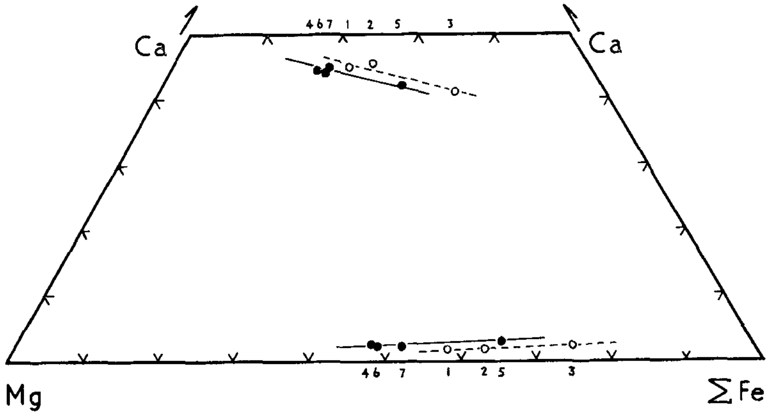

Fig. 5. Triangular plot of pyroxene compositions based on atomic per cent of calcium, magnesium, and total iron plus manganese (ΣFe). Compositional trends for pyroxenes from the two higher-grade subzones are worked by full lines, those for the lower-grade subzone by dashed lines. These illustrate the increase found in mutual solid solution with increase in iron content of the pyroxenes, and the tendency for mutual solid solution to increase with grade.

positions from which the extent of mutual solid solution between lime-rich monoclinic and lime-poor orthorhombic phases may be determined. The relatively small quantities of aluminium, titanium, and alkalis are ignored. On such a plot (fig. 5) the Broken Hill clinopyroxenes coexisting with orthopyroxene describe a compositional trend sloping away from the diopside–hedenbergite join towards the orthoferrosilite corner, that is, a trend of increasing solid solution of orthopyroxene with increasing iron content. A line has been drawn between clinopyroxenes 4, 6, and 7 (which plot very close) and clinopyroxene 5, representing the trend of clinopyroxene compositions in the two higher subzones of the granulite zone at Broken Hill (full line on fig. 5). Clinopyroxenes 1 and 2 from the lower-grade subzone plot distinctly to the lime-rich side of this trend line, and although clinopyroxene 3 is too far removed from the remainder to permit definite distinction, there is a suggestion that the compositional trend line of the lower-grade clinopyroxenes (dashed line on fig. 5) lies to the lime-rich side of that for the higher grades, implying an increase in the extent of solid solution of orthopyroxene by clinopyroxene with increase in metamorphic grade. Similarly orthopyroxenes 1, 2, and 3 lie to the lime-poor side of a compositional trend line passing through orthopyroxenes 4, 5, 6, and 7 from the two higher-grade subzones, likewise suggesting an increase in the extent of solid solution of clinopyroxene by orthopyroxene. There is also a tendency for iron-rich orthopyroxenes to show more solid solution relative to magnesian ones.

The increased solid solution of the other pyroxene phase exhibited by iron-rich members of both orthopyroxene and clinopyroxene series relative to the magnesium members formed under similar temperature conditions is consistent with crystal chemical considerations. The ionic radius of $Fe^{\cdot\cdot}$ being closer to $Ca^{\cdot\cdot}$ than is that of $Mg^{\cdot\cdot}$, ferrous iron more readily replaces calcium in the octahedrally coordinated site than does magnesium, so that the solvus curve is lower in the iron-rich portions of the pyroxene phase diagram than in the magnesian. Increase in solid solution between isomorphous compounds of limited miscibility is a common consequence of increase in equilibrium temperature, and although they are not strictly isomorphous, it is most interesting to observe a tendency towards increased solid solution with increase in metamorphic grade between the two pyroxene phases in basic granulitic rocks at Broken Hill.

Summarizing, then, there are two consequential effects of increase in metamorphic grade upon coexisting orthopyroxene–clinopyroxene assemblages; first the distribution relationship of ferrous iron and magnesium in the two phases alters so that ferrous iron becomes relatively more concentrated in the clinopyroxene (fig. 4), and secondly mutual solid solution between the two pyroxenes tends to increase (fig. 5). Neither is illustrated in an entirely ideal fashion by the Broken Hill data but each is sufficiently distinct to be established in principle.

General considerations on ferrous-iron–magnesium distribution in pyroxenes.

On a distribution diagram with respect to ferrous iron and magnesium, a curve representing orthopyroxene and clinopyroxene coexisting under equilibrium conditions in higher-grade regional metamorphic rocks has been established by Mueller (1960, 1961) and Kretz (1961). Its shape has been assumed to indicate ideal solid solution with respect to ferrous iron and magnesium in the two pyroxene series, that is, in assemblages of differing bulk chemistries the standard reaction (following Bartholomé, 1961): Diopside + orthoferrosilite $\rightleftharpoons$ hedenbergite + enstatite will proceed until concentrations of iron and magnesium in the members of the various coexisting pyroxene pairs obey a relationship of the form[1] $(\mathrm{Fe}^{\cdot\cdot}/\mathrm{Mg}^{\cdot\cdot})_{opx} = K.(\mathrm{Fe}^{\cdot\cdot}/\mathrm{Mg})_{cpx}$ where K, the distribution coefficient, is constant over all variations in iron and magnesium contents for the given equilibrium conditions.

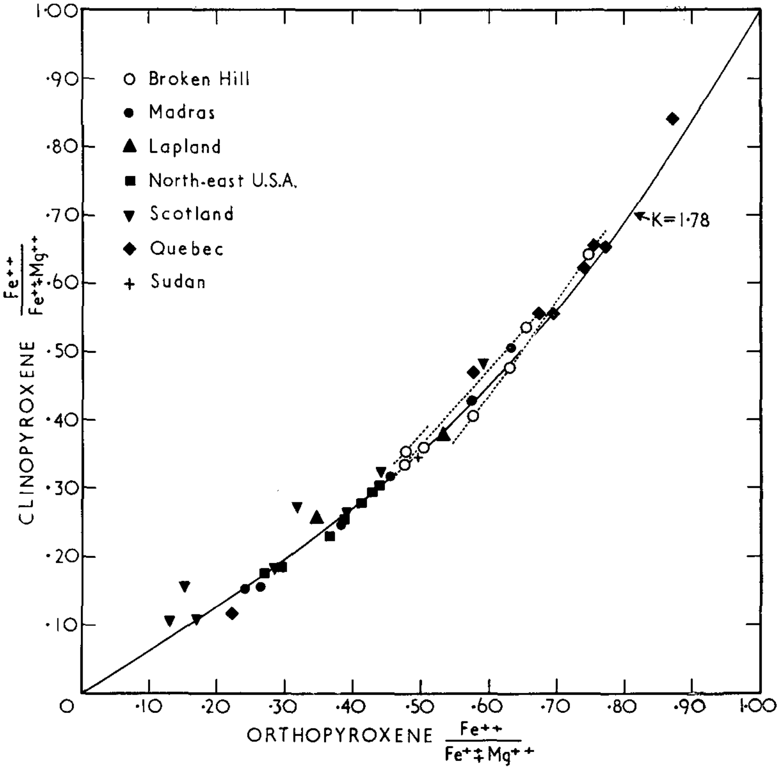

FIG. 6. Distribution diagram for coexisting pyroxenes from high-grade regional metamorphic terrains (atomic ratio $\mathrm{Fe}^{\cdot\cdot}/(\mathrm{Fe}^{\cdot\cdot}+\mathrm{Mg})$ for orthopyroxene plotted against that of clinopyroxene). An averaged distribution curve ($K = 1{\cdot}78$) based on the ideal solid solution theory is drawn (solid curve), also the distribution trends at Broken Hill (dotted lines). Sources of data: Broken Hill, this paper; Madras, Howie (1955); Lapland, Eskola (1952); North-east U.S.A., Clavan, McNabb, and Watson (1954), Norton and Clavan (1959); Scotland, Muir and Tilley (1958), O'Hara (1960, 1961*a*, 1961*b*); Quebec, Krank (1961); Sudan, Howie (1958).

[1] The same relationship has been expressed in an inverted form by Kretz (1961) and Mueller (1960). Bartholomé's notation is preferred here for its simplicity and because it produces plots directly comparable with optical plots and is consistent with the conventional procedure of placing magnesian end-members on the left-hand side of diagrams.

In fig. 6 all satisfactory analyses of clinopyroxene–orthopyroxene pairs from high-grade regional metamorphic terrains known to the writer have been plotted on such a distribution diagram, together with a curve representing an averaged distribution coefficient $K = 1{\cdot}78$. Departure of individual pairs from the average curve in terms of distribution coefficient is substantial; actual values of K range from 1·3 to 2·2.

It is perhaps significant that towards the magnesian end of the curve the majority of pyroxene pairs fall on or slightly below the curve, whilst more iron-rich pairs fall on or slightly above the curve.[1]

If this observation is not simply due to an insufficiency of data, it denotes some second-order variation in the distribution relationships between coexisting pyroxenes dependent upon composition. Mueller (1961) describes S-shaped distribution curves resulting from regular solid solution instead of ideal solid solution relationships in cummingtonite, and an analogous situation perhaps occurs in one or other of the pyroxene series, especially the clinopyroxenes.

Similarly, plotting $Fe^{\cdot\cdot}/Mg^{\cdot\cdot}$ of orthopyroxene against that of clinopyroxene, the line of best fit is a slightly curved line rather than the straight line theoretically predicted on the ideal solid-solution model.

The manner in which the Broken Hill pyroxenes plot also suggests a slight departure from an ideal solid-solution relationship. On the distribution diagram of figs. 4 and 6 the trends defined by analysed pairs from the lower- and intermediate-grade subzones, substantiated by abundant optical information, do not lie parallel to the curve representing $K = 1{\cdot}78$ but intersect it at a small angle. On a $Fe^{\cdot\cdot}/Mg^{\cdot\cdot}$ plot for orthopyroxene versus clinopyroxene (fig. 7), the three analysed pairs from the lower-grade subzone (1, 2, 3) fall on a straight line which does not pass through the origin. The line defined by pyroxene pairs from the intermediate subzone is parallel to this and also does not pass through the origin. Since pair 7 appears anomalous, little can be concluded concerning the trend in the higher-grade subzone except that it lies above the intermediate and low subzone trends.

From thermodynamic considerations, Kretz (1961) concludes that the distribution coefficient, K, is a function of temperature and pressure, and is relatively independent of compositional variations. The information from Broken Hill, however, shows that at constant temperature

---

[1] Magnesian pair X819 (O'Hara, 1961*b*) from Scourie comes from a zoned contact gneiss. The analysed clinopyroxene is a heavy fraction, and the orthopyroxene a light fraction, so that the point denoting these pyroxenes on fig. 6, falling well above the distribution curve, probably does not represent a strictly coexisting pair.

and pressure conditions a distribution coefficient of this form is not invariant, but depends on composition; for instance, K ranges from 1·99 in magnesian pair 1 to 1·68 in iron-rich pair 3 within the lower-grade subzone. Rather, the parallelism of the trends for the lower- and intermediate-grade subzone pairs on fig. 7 suggests the applicability at Broken Hill of an empirical distribution relationship:

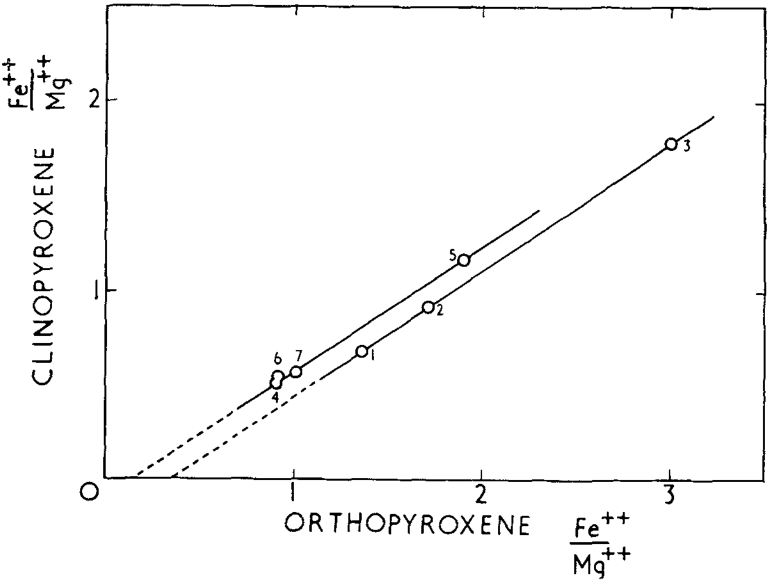

FIG. 7. Plot of atomic ratio $Fe^{\cdot\cdot}/Mg^{\cdot\cdot}$ for orthopyroxene against that of coexisting clinopyroxene, with distribution trends for the lower-grade (1, 2, 3) and intermediate-grade (4, 5) subzones.

$$(Fe^{\cdot\cdot}/Mg)_{opx} = P + Q(Fe^{\cdot\cdot}/Mg)_{cpx}$$

where now Q is a constant for all equilibrium conditions (defined by the slope of the distribution line on a $Fe^{\cdot\cdot}/Mg^{\cdot\cdot}$ plot such as fig. 7, and equal to 1·48 approximately) and P is a function of metamorphic grade (measured by the intercept of the distribution line with the orthopyroxene axis on fig. 7); P varies from 0·35 to 0·17 between the lower-grade and intermediate-grade subzones of the zone of hornblende–pyroxene granulites at Broken Hill.

This equation, however, clearly cannot be reconciled with the pyroxene pairs from other regions plotted on the distribution diagram of fig. 6

unless it happens that magnesian assemblages with co-existing pyroxenes represent as a whole higher grades of metamorphism than iron-rich assemblages. Consulting the description of the iron-rich pyroxene assemblages from Quebec one finds that 'the surrounding gneisses are muscovite-biotite gneisses and other rocks typical of migmatised areas of the amphibolite facies' (Krank, 1961). On the other hand, for the Lewisian rocks of Scourie where coexisting pyroxene assemblages are relatively magnesian, M. J. O'Hara (priv. comm.) suggests metamorphism at higher temperatures than occurred in the Madras and Ceylon charnockite–granulite provinces, basing this conclusion on comparison of primary feldspar chemistry. At Broken Hill, the abundance of hornblende in basic rocks and of biotite in acid and the proximity of a zone of amphibolite facies rocks indicate a somewhat lower grade of metamorphism (hornblende–granulite subfacies) than in other granulite terrains. Thus, stability fields of coexisting pyroxenes appear to depend on the iron : magnesium ratio of the parent rock; that is, under given temperature and pressure conditions only those coexisting pyroxene pairs within a relatively limited iron–magnesium compositional field are stable.

It would remain to be explained why coexisting pyroxene assemblages from all granulitic terrains should be restricted within such narrow limits on the distribution diagram of fig. 6 or on a similar diagram corresponding to fig. 7; if the empirical distribution relationship suggested above is the only restriction placed upon pyroxene assemblages, why should there be no iron-rich assemblages in high-grade areas like Scourie plotting well above the distribution curve of fig. 6, and why no magnesian assemblages in low-grade areas such as Quebec plotting well below the curve? The extent to which mineral reactions such as the breakdown of amphiboles to pyroxenes, and the reaction of orthopyroxene with plagioclase to form clinopyroxene plus garnet, are dependent upon iron–magnesium ratios is at present unknown, for so little data exists on the chemistry of these assemblages. It would seem a great coincidence that under the temperature and pressure conditions of high-grade regional metamorphism, mineral reactions such as the above should be just so dependent upon iron–magnesium composition as to produce a fortuitous distribution curve of the ideal solid-solution type. In hornfelses and in igneous rocks pressure conditions may prohibit reaction of orthopyroxene and plagioclase to form clinopyroxene and garnet, so that iron-rich pyroxene pairs may occur at higher temperatures than in granulitic rocks, and in consequence their iron–magnesium distribution will result in their 'anomalously' plotting off the granulitic distribution curve (cf. the hornfels pyroxene pairs of Muir and Tilley (1958) discussed by Kretz, 1961, page 376). Many pyroxene hornfels have been formed under sanidinite facies conditions at rather higher temperatures than occurred in either pyroxene hornfels facies or normal granulite facies conditions, so it is not surprising that they do not obey the distribution laws applicable to granulite pyroxenes.

It is most interesting to observe that igneous pyroxene pairs approximately satisfy the relationship $(\mathrm{Fe}^{\cdot\cdot}/\mathrm{Mg}^{\cdot\cdot})_{opx} = P+Q(\mathrm{Fe}^{\cdot\cdot}/\mathrm{Mg}^{\cdot\cdot})_{cpx}$ with a value of Q similar to that of Broken Hill rocks (1·44 for the igneous pyroxenes quoted by Kretz, 1961) and P equal to zero.

In the foregoing it has been shown that the distribution of iron and magnesium between coexisting pyroxenes in granulites from Broken Hill contradicts the theoretical conclusions based on thermodynamical consequences of an ideal solid-solution theory. An alternative consistent with the Broken Hill data has been proposed, but it is unsubstantiated by theory and is based on an absolute minimum of data. Clearly much more chemical information on coexisting pyroxene assemblages is required before we can fully understand the distribution relationship of iron and magnesium in coexisting pyroxene assemblages.

As a possible explanation of the discrepancy between the observed distributional relationships and the ideal situation presented by Kretz and others, the writer suggests that the calcium content of clinopyroxenes, i.e. the extent of solid solution between orthopyroxene and clinopyroxene, should not be ignored. Changes in other sites of the pyroxene structure may influence appreciably the distribution of cations in the iron–magnesium site, especially if there is a preferential acceptance of magnesium or iron (notably the latter) into the calcium site of the clinopyroxene as a result of orthopyroxene solid solution. The difference between iron-rich and magnesian pyroxene pairs in the extent of mutual solid solution of clinopyroxene and orthopyroxene, and the changes in these extents with temperature and pressure conditions, would then affect overall iron–magnesium distribution considerably. Another possible explanation, suggested in a personal communication by Bartholomé, is the ordering of Fe and Mg in the pyroxene structure and temperature dependence of the degree of order.

Value of coexisting pyroxenes as indicators of metamorphic grade.

Despite current uncertainties regarding the precise theoretical relationships concerned in cation distribution, the use of coexisting pyroxenes as indicators of metamorphic grade holds definite promise. The present paper records one example of a metamorphic terrain where it has proved possible to detect differences dependent upon metamorphic grade in the optical property relationships between coexisting pyroxenes, and where differing distribution relationships of the major components have been revealed as the underlying chemical factors. The sensitivity attainable by modern analytical techniques appears sufficient to detect the changes concerned.

In his study of pyroxene assemblages from a thermodynamic viewpoint based on the ideal solid-solution model, Kretz (1961) has concluded that temperature dependence of the cation distribution relationship dominates pressure dependence, and with this as first approximation the dominance probably extends to more complex solution models. Variation in pressure conditions during metamorphism over that portion of the Broken Hill region under discussion in this paper is unlikely to have been great, so that the changes in metamorphic grade defined either by new mineral assemblages or by changes in cation distribution will principally reflect changes in temperature of crystallization. This suggests that if the nature of distribution relationships in coexisting pyroxenes eventually proves useful, the method will find its most valuable application in problems of geological thermometry. It will by no means be restricted to the study of regional metamorphic rocks but will also be applicable to the investigation of other solid–solid and liquid–solid equilibrium assemblages, i.e. to contact metamorphic and igneous rocks.

It is hoped that the present contribution will stimulate further geochemical studies of pyroxene assemblages, particularly in other regions where the metamorphic zonal sequence is established, leading to the accumulation of data that must be the next step before further progress in this subject is made. The advent of this data will either prove or disprove the general feasibility of using cation distribution between pyroxenes as an indication of grade or as a geological thermometer, and if the former, the empirical and perhaps the theoretical principles underlying cation distribution will become clearer.

Acknowledgements. The writer is grateful to Prof. C. E. Tilley and Dr. S. R. Nockolds for their interest and encouragement during the progress of this work, and thanks them and Dr. I. D. Muir for reading and discussing the manuscript. The use of facilities in the Department of Mineralogy and Petrology, Cambridge, where analyses of Broken Hill pyroxenes were carried out, is also gratefully acknowledged.

References.

BARTHOLOMÉ (P.), 1961. Geol. Mag., vol. 98, p. 346.

CLAVAN (W.), McNABB (W. M.), and WATSON (E. H.), 1954. Amer. Min., vol. 39, p. 566.

ESKOLA (P.), 1952. Amer. Journ. Sci., Bowen vol., p. 133.

FYFE (W. S.), TURNER (F. J.), and VERHOOGEN (J.), 1958. Geol. Soc. Amer. Memoir 73.

HOWIE (R. A.), 1955. Trans. Roy. Soc. Edin., vol. 62, p. 725.

—— 1958. Service Géol. Congo Belge, Bull. 8, Fasc. 2.

KING (H. F.) and THOMSON (B. P.), 1953. Proc. Fifth Emp. Min. Met. Cong., vol. 1, p. 533.

KRANK (S. H.), 1961. Journ. Petr., vol. 2, p. 137.

KRETZ (R.), 1961. Journ. Geol., vol. 69, p. 361.

MUELLER (R. F.), 1960. Amer. Journ. Sci., vol. 258, p. 449.

—— 1961. Geochimica Acta, vol. 25, p. 267.

MUIR (I. D.) and TILLEY (C. E.), 1958. Geol. Mag., vol. 95, p. 403.

NORTON (D. A.) and CLAVAN (W. S.), 1959. Amer. Min., vol. 44, p. 844.

O'HARA (M. J.), 1960. Geol. Mag., vol. 97, p. 145.

—— 1961*a*. Min. Mag., vol. 32, p. 848.

—— 1961*b*. Journ. Petr., vol. 2, p. 248.